Science of the Total Environment 918 (2024) 170786

Contents lists available at ScienceDirect

Science of the Total Environment

journal homepage: www.elsevier.com/locate/scitotenv

Diurnal patterns of spatial stream temperature variations reveal the need for integrating thermal heterogeneity in riverscape habitat restoration

Joachim Pander [a], Johannes Kuhn [a], Roser Casas-Mulet [a,b], Luis Habersetzer [a], Juergen Geist [a,*]

[a] Aquatic Systems Biology Unit, TUM School of Life Sciences, Technical University of Munich, 85354 Freising, Germany
[b] Chair of Hydraulic and Water Resources Engineering, Technical University of Munich, 80333 Munich, Germany

HIGHLIGHTS

- Spatio-temporal temperature heterogeneity was characterized in a large restored riverscape.
- Diurnal temperature variations of up to 14 °C were detected, exceeding species tolerances.
- Groundwater influence, shading and bed morphology were key factors governing patchiness.
- Greatest resilience was associated with thermal mosaics of dynamic and complex riverscapes.
- Providing thermal refuges and connectivity should be key priorities in mitigating heat stress.

GRAPHICAL ABSTRACT

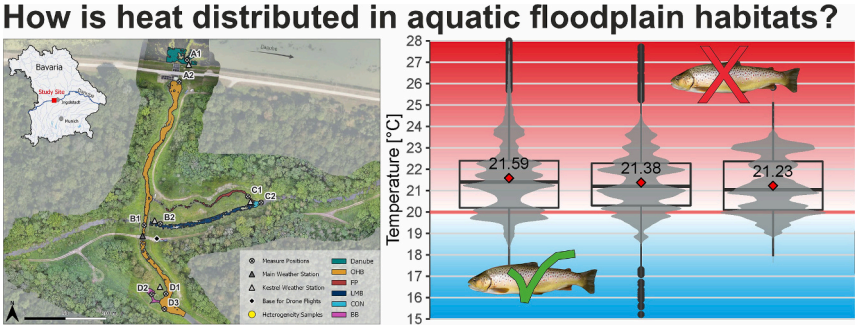

ARTICLE INFO

Editor: Daniel Wunderlin

Keywords:
Thermal heterogeneity
Global warming
Remote sensing
TIR-imagery
River restoration
Cold-water fish
Cold-water refuges

ABSTRACT

Longer durations of warmer weather, altered precipitation, and modified streamflow patterns driven by climate change are expected to impair ecosystem resilience, exposing freshwater ecosystems and their biota to a severe threat worldwide. Understanding the spatio-temporal temperature variations and the processes governing thermal heterogeneity within the riverscape are essential to inform water management and climate adaptation strategies. We combined UAS-based imagery data of aquatic habitats with meteorological, hydraulic, river morphology and water quality data to investigate how key factors influence spatio-temporal stream heterogeneity on a diurnal basis within different thermal regions of a large recently restored Danube floodplain. Diurnal temperature ranges of aquatic habitats were larger than expected and ranged between 14.2 and 28.0 °C (mean = 20.7 °C), with peak median temperatures (26.1 °C) around 16:00 h. The observed temperature differences in timing and amplitude among thermal regions were unexpectedly high and created a mosaic pattern of temperature heterogeneity. For example, cooler groundwater-influenced thermal regions provided several cold water patches (CWP, below 19.0 °C) and potential cold water refuges (CWRs) around 12:00 h, at the time when other habitats were warmer than 21.0 °C, exceeding the ecological threshold (20.0 °C) for key aquatic species. Within the morphological complexity of the restored floodplain, we identified groundwater influence, shading and river morphology as the key processes driving thermal riverscape heterogeneity. Promoting stream thermal refuges will become increasingly relevant under climate change scenarios, and river restoration should consider both measures to physically prevent habitat from excessive warming and measures to improve connectivity that

* Corresponding author.
E-mail address: geist@tum.de (J. Geist).

https://doi.org/10.1016/j.scitotenv.2024.170786
Received 22 August 2023; Received in revised form 25 January 2024; Accepted 5 February 2024
Available online 6 February 2024
0048-9697/© 2024 The Authors. Published by Elsevier B.V. This is an open access article under the CC BY license (http://creativecommons.org/licenses/by/4.0/).

meet the temperature requirements of target species for conservation. This requires restoring mosaics of complex and dynamic temperature riverscapes.

1. Introduction

Temperature is a critical driver of habitat functioning in rivers and streams (Steel et al., 2017), governing key physico-chemical habitat variables such as oxygen availability for aquatic biota (Piatka et al., 2022), and biological processes such as productivity and decomposition (Leclerc et al., 2023). In this context, temperature is not only linked to the trophic status of an aquatic system (Poff et al., 2002), but it also drives the physiology (Pörtner and Peck, 2010) and the resistance of the immune system of aquatic biota against infections (Messina et al., 2023). It also triggers key processes within species' life cycles such as the timing of emergence for macroinvertebrates (Piggott et al., 2015), and spawning times for fish (Kaylor et al., 2021). The continued longer durations of heat periods, altered precipitation, and modified streamflow patterns driven by climate change are expected to increase negative pressures of water scarcity and temperature stress in freshwater ecosystems (White et al., 2023), exposing rivers and their biota to a severe threat worldwide (Reid et al., 2019; Vörösmarty et al., 2010). Land-use changes, water extractions, and stream regulation increase the susceptibility to such alterations of rivers and their corridors, exemplified by increased drought severity, higher stream temperatures, and habitat degradation (Geist and Hawkins, 2016; Van Vliet et al., 2013). Such unprecedented changes and synergies of multiple stressors (Bierschenk et al., 2019; Wild et al., 2023) call for action to develop effective river restoration measures that go far beyond classical restoration approaches (e.g. Castro and Thorne, 2019; Johnson et al., 2020; Powers et al., 2022; Wohl et al., 2021). These typically target restoring connectivity or geomorphological patterns in riverscapes to support freshwater ecosystem resilience in cold and temperate climates (Geist, 2015; Gilvear et al., 2013; McCluney et al., 2014; Skidmore and Wheaton, 2022; Wilby et al., 2010).

Thermal heterogeneity within riverscapes is increasingly considered an essential aspect of river habitat quality, given its capacity to provide cold water patches (CWPs, Casas-Mulet et al., 2020; Kuhn et al., 2021) as potential cold water refuges (CWRs, Mejia et al., 2023) during summertime. The availability of CWPs is important when temperature tolerances of certain aquatic species are exceeded (Casas-Mulet et al., 2020; Kuhn et al., 2021), particularly as summer periods are increasingly warmer, globally (Kaushal et al., 2010; Orr et al., 2015; Van Vliet et al., 2013). Rivers are complex dynamic ecosystems with their physical structure represented as a hierarchical organisation of interconnected spatial scales (Braun et al., 2012; Thorp et al., 2006; Wohl, 2016; Wohl et al., 2021). Whilst river temperature is driven by subsurface interactions in the hyporheic zone (Brunke and Gonser, 1997) in combination with climatic, topographic, and hydrological controls at the air-water interface (Caissie, 2006; Webb et al., 2008; Daniels and Danner, 2020; Siegel et al., 2022), an array of physical features determine how heat is distributed (Carbonneau et al., 2012; Dugdale et al., 2015; Fausch et al., 2002; Poole et al., 2006). Stream thermal heterogeneity is, therefore, the result of a spatial interplay of dynamic groundwater inputs (Arrigoni et al., 2008; Dugdale et al., 2013; Poole et al., 2006; Dal Sasso et al., 2021), in-channel physical complexity (Sawyer and Cardenas, 2012; Tonolla et al., 2010), and shading (Garner et al., 2017; Torgersen et al., 1999).

Understanding the processes governing thermal heterogeneity within the riverscape are essential to inform water management targets in climate adaptation strategies (Keppel et al., 2015; Morelli et al., 2016; Palmer et al., 2008; Fullerton et al., 2018; Isaak et al., 2015; Kurylyk et al., 2015; Torgersen and Ebersole, 2012; Mejia et al., 2023). The spatial changes in stream thermal heterogeneity are key not only on an annual scale, where large temperature differences between aquatic habitats are expected, but also on higher-resolution temporal scales (e.g. diurnal), where variations between and within habitats across rivers are less studied. Thermally differentiated habitats or cold water patches (CWPs, Casas-Mulet et al., 2020; Kuhn et al., 2021) can determine the availability of cold water refugia for species (CWPs can become CWRs when used by organisms to survive temperature stress, Mejia et al., 2023). The availability of CWRs can largely drive aquatic species short-term movements, migration, feeding strategies and reproduction behaviour, and promote their long-term persistence (Armstrong and Schindler, 2013; Kuhn et al., 2021). Warmer water temperatures that diversify the thermal landscape may also favour aquatic species (Armstrong et al., 2021), particularly since warmer water can lead to faster growth, which is an important proxy e.g. for the survival of fishes. Therefore, mapping diurnal thermal patterns at large spatial scales is critical to determine overall riverscape habitat quality and inform river restoration strategies to promote climate-change resilient freshwater ecosystems.

Uncrewed Aerial Systems (UASs) – or drones – equipped with Thermal Infra-Red (TIR) cameras provide small, inexpensive, fast, and flexible solutions to obtain high-resolution stream thermal imagery (Dugdale, 2016; Fullerton et al., 2018; Steel et al., 2017). Such technological developments have supported extensive investigations of stream spatial thermal heterogeneity in the last decade. They include studies within stream channels (e.g. Torgersen et al., 2001; Ebersole et al., 2003; Dugdale et al., 2013; Eschbach et al., 2017; Fullerton et al., 2018), across floodplains (Tonolla et al., 2010), and along riverscapes (Casas-Mulet et al., 2020; Dugdale et al., 2015; Handcock et al., 2012; Wawrzyniak et al., 2013), with few studies providing simultaneous stream temperature and physical habitat imagery (but see e.g. Casas-Mulet et al., 2020; Kuhn et al., 2021). However, multi-temporal assessments of thermal heterogeneity are rare. In particular, diurnal variations in stream temperature using high-resolution imagery are barely considered so far (but see Wawrzyniak et al., 2013, three to four flights per day and Tonolla et al., 2010, 12–15 min intervals over 24 h cycles). In addition to spatial patterns of temperature, temporal variations are equally important, particularly in a global warming environment with increased thermal maxima in frequency and duration (Wild et al., 2023).

Key gaps in knowledge include understanding how daily changes in stream temperatures impact ecological processes, and specifically the role of innovative remote sensing tools to assess such changes and support conservation management efforts in freshwater systems. Addressing such gaps is key to identifying and prioritising river restoration measures at the reach and riverscape scales (Letcher et al., 2016). Taking advantage of the current advances in aerial data acquisition (Huang and Zeng, 2017; Maes and Steppe, 2019; Dugdale et al., 2019; Casas-Mulet et al., 2020; Kuhn et al., 2021; Mishra et al., 2023), we employed UASs equipped with TIR and RGB cameras to obtain high-resolution stream thermal and physical habitat imagery simultaneously (see Casas-Mulet et al., 2020). Our aim was to understand how stream thermal heterogeneity varies across high spatio-temporal resolutions, and the potential consequences for freshwater biota, which may need to be considered in management of aquatic systems under future climate scenarios. Since this is not only important during low flow conditions when warming up of riverine habitats is likely, we used thermally differentiated aquatic habitats during regular flow conditions as suggested by White et al. (2023) in one of the most important floodplain restorations along the Danube to answer the following scientific questions:

(i) What is the daily range of stream temperatures within and between a complex mosaic of thermal habitats along a representative riverscape?
(ii) How do key meteorological, morphological and hydrological factors influence stream thermal heterogeneity?

2. Material and methods

2.1. Study site

The study area is located in a restored floodplain of the upper River Danube near Ingolstadt, southern Germany, within one of the largest remaining alluvial forests in the Danube system (Fig. 1; River Danube, river kilometre 2472; Stammel et al., 2012). The Bavarian Danube is part of the barbel region (*Barbus barbus* L.), with dominating fish species from the guild of current-adapted cyprinids, but also cold-water adapted salmonids such as European grayling (*Thymallus thymallus* L.), brown trout (*Salmo trutta fario* L.) and Danube salmon (*Hucho hucho L.*) (Leuner et al., 2013). The restored floodplain is fed through an artificial diversion of surface water, the Ottheinrichbach channel (OHB), taking water from the Danube above the Ingolstadt power plant (Pander et al., 2019). Parallel to the Danube mainstream, the Längenmühlbach (LMB) channel serves as a groundwater-fed hinterland drainage for the Danube dykes, which displays cooler water temperatures in summer and warmer in winter (Pander et al., 2023). The OHB crosses the LMB in the study area by means of a trough bridge and only connects to it through a fishpass channel (FP). After the intersection with the fishpass, the LMB flows into the Danube in the tailwater of the power plant Bergheim (Fig. 1, 48°44′55.7 N, 11°16′35.7 E). In addition to the Danube River and numerous channels, various sizes of stagnant water bodies are distributed over the floodplain, creating a variety of waters with different structural properties potentially comprising unique temperature regimes and promoting thermal heterogeneity within this floodplain system (Fig. 1). Based on the well-known structural habitat heterogeneity in this system (Pander et al., 2018), this study targeted several thermal regions within the restored floodplain consisting of bank habitat of the Danube, OHB, LMB, FP that is connecting LMB and OHB, Floodplain pond (Billabong, BB) that is connected to the OHB, and confluence section of LMB and FP (CON, Fig. 1).

The upper Danube along the study area is characterized by a slow-flowing channel, classified as a highly modified water body, mainly due to hydropower generation activity and flood protection works. Its cross-section profile is double-bermed, creating an approximately 30 m wide shallow area along the embanked river banks with a uniform water depth of <1 m and little current speed. Bank vegetation or other means of shading are minimal in this location of the Danube mainstream. The OHB originates from the warm surface water of the Danube and has no groundwater influence, in contrast to the LMB. The OHB comprises a large diversity of current speed, water depth, and patchy macrophytes, and it is partly shaded by overhanging shrub vegetation. The Danube's surface water largely drives stream temperature in the OHB. The BB is a billabong-like aquatic habitat connected to the OHB. It comprises steep banks, dense macrophytes, medium depth (maximum of 1.5 m), slow water velocities and a water body fully exposed to the sun. The LMB is a

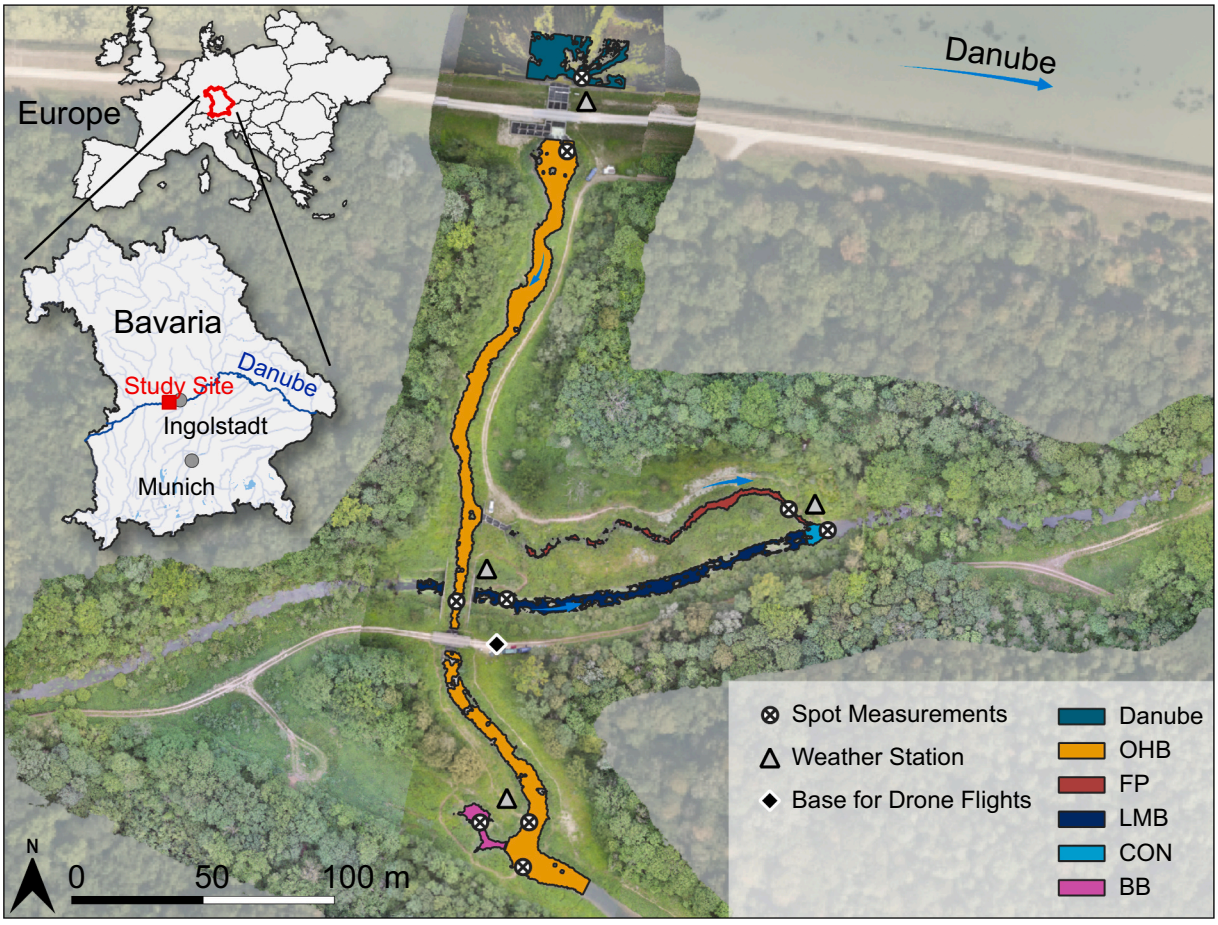

Fig. 1. Study area within Bavaria, Germany, and location of the floodplain restoration at the Danube. Sketch includes a schematic top-view on the different investigated thermal regions with location of the measuring spots for the meteorological, morphological and hydrological factors as well as spatio-temporal resolved temperature measurements, the base for drone flights and the used weather stations. Danube = represents the main stem of the Danube, OHB = Ottheinrichbach, FP = fish pass, LMB = Längenmühlbach, CON = confluence between fishpass and Längenmühlbach, BB = billabong connected to the OHB.

channel-like small river that originates besides draining water from agricultural land use, mostly from upwelling cool groundwater. The high groundwater influence in the LMB is the main reason for its low O_2 saturation and high EC. Due to the clear water in this river, a high density of macrophytes occurs. The LMB steep banks are stabilised with bank riprap covered with riparian vegetation of elders and willows, which partly shade the small stream. The FP has its origin in the OHB. Its structure is a subsequent changing sequence of small pools and riffles that are all interconnected to allow up and downstream fish movement. The CON is the mixing zone between the groundwater-influenced LMB and the FP fed by surface water from the Danube via the OHB. Its river morphological character is the same as in the LMB.

2.2. Data acquisition and processing

We combined UAS-based imagery data with meteorological, hydraulic, river morphology and water quality point data to investigate how the latter influence spatio-temporal stream heterogeneity in the study area. The data acquisition took place at a typical summer day with average indicative outside temperatures of close to 30 °C – a situation which is meanwhile typical for the climatic regime of this region under the climate change scenario. However, it has to be stated that during summer, temperature maxima of 36 °C and more are reached.

2.2.1. UAS-based imagery data acquisition

We used a UAS (Matrice 200, DJI, Shenzhen, China) equipped with a thermal and visual spectrum camera (Zenmuse XT2 (640 × 512 pixels thermal), DJI, Shenzhen, China) and flew hourly under almost cloud-free conditions (warm and stable summer weather) from 6:00 to 20:00 h on 20 July 2020, resulting in 16 flight missions. Four Hobo® temperature loggers (UA-002-064 HOBO, Onset Computer Corporation, Bourne (MA), USA) were used to record reference temperatures in addition to the temperature loggers installed at each measuring point, as the basis for TIR imagery calibration. Those four loggers recorded the water temperature in one-minute intervals and were placed in spatial proximity to the flight base, one inside a cold white box filled with ice and water (~0 °C; cold reference) and one in a warm black box filled with warmed water (~50 °C; warm reference). In addition, one logger was placed directly in the OHB, and the fourth one was placed in the LMB so that all loggers could be captured in one TIR image (Fig. 1). Nine temperature loggers (UA-002-064 HOBO, Onset Computer Corporation, Bourne (MA), USA) were installed at 5 mm below the water surface logging at 1 min intervals to enable further TIR data calibration (when required), and validation. All loggers were installed before the UAS flights and retrieved at the end of the day. Two experienced drone pilots carried out automated mission flights (mode for mapping, DJI based) for every single flight event using the same automated flight mode. The UAS flew 50 m above the ground at a speed of 2.5 m/ s, collecting images at a 90 % longitudinal and 80 % transversal overlap between adjacent images along and across the river, producing ~352 individual outputs of each RGB and TIR imagery per flight mission. The average time of each automated flight campaign was approximately 15 min, and the covered area was 18,260 m^2.

2.2.2. UAS-based imagery data processing

Desktop-based processing encompassed TIR thermal calibration by calculating linear models. To calibrate raw imagery with the ground-truth data, we extracted the pixel temperature data (3 × 3 pixels area) of each flight TIR image at the reference logger position (cold-reference, warm-reference and the Loggers in OHB and LMB) using Thermography software (FLIR Tools, Teledyne FLIR LLC, Wilsonville, Oregon, USA). In the next step, we assessed reference logger temperatures using HOBOware (Onset, Bourne, Massachusetts, USA) to export the outcome as a CSV file. Linear models (mean $R^2 = 0.99$, $\pm SD = 0.002$ for models used) were computed to calibrate the different temperature codes in TIR images for each mission flight separately with the field temperature measurements of the reference logger to the respective time point of the flight. We converted each flight's TIR imagery to CSV files using R-studio (www.rstudio.com/categories/rstudio-ide/, last accessed 31 July 2023) to enable the application of the linear model for thermal calibration, and then data were exported back to image files using Matlab (MathWorks, Natick, Massachusetts, USA). The calibrated TIR-images were then merged into a single orthomosaic using photogrammetry software (Agisoft Photoscan Professional, Agisoft LLC, St. Petersburg, Russia) and created the basis for further spatial analysis. Reference ground control points (GCPs), clearly identifiable in both TIR and RGB imagery, were referenced from Bayernatlas (https://geoportal.bayern.de/bayernatlas/?lang=de&topic=ba&bgLayer=atkis&catalogNodes=11, last accessed 31 July 2023) and their coordinates were used for georeferencing and allow overlapping between both imagery sets. We used a combination of thermal and optical RGB data to distinguish water temperature pixels from terrestrial temperature pixels as described in Kuhn et al. (2021). To do so, we merged RGB images into a single orthomosaic of one representative flight mission (flight mission at 13:00 h) with the same software as the TIR images and classified them to water surface, macrophytes breaking through water surface or terrestrial origin, based on spectral properties using geoinformatics software (Arcmap 10.5, ESRI, Redlands (CA), USA). In the final step, the created orthomosaic was overlaid with the delineation of fluvial thermal regions Danube, OHB, LB, BB and CON. Imagery spatial resolution was 0.23 m per pixel in the TIR-imagery and 0.035 m per pixel in the RGB-imagery. Temperature data was exported as raster data for each thermal region for further statistical analyses. Since the data of the flight at 10:00 h could not be recorded reliably, this flight was omitted from the data set.

2.2.3. Point data acquisition

Four Kestrel® 4500 Pocket Weather® Tracker weather stations (Kestrel, Birmingham, Minnesota, USA) were used to measure small-scale weather changes throughout the day. These were mounted on tripods to rotate freely with wind vanes so that they could correctly measure the parameters (temperature [°C], wind direction [°], wind speed [m/s], humidity [%]). The weather stations were calibrated by logging for 80 min in one location so they were all exposed to equal conditions and recorded data could be corrected at a later stage. The mean value of the data for each station was then calculated from the calibration measurement data, and the respective offset to the mean value of all four stations was derived. This offset was used to correct the data set of the diurnal survey, whereby the corrections were small (Standard deviation (SD) of temperature: ±0.04 °C, wind direction: ±9.1°; wind speed: ±0.02 $m \cdot s^{-1}$, humidity: ±2.95 %).

To avoid time lags between measuring physico-chemical point data and drone flights (Letcher et al., 2016), these data were measured simultaneously to each flight in situ at the respective thermal regions in the open water column of the river at each of the 9 spot measurements (Fig. 1). Dissolved oxygen [$mg \cdot L^{-1}$], temperature [°C], electrical conductivity [$\mu S \cdot cm^{-1}$, corrected to 20 °C], and pH were measured with a hand-held WTW® Multimeter 340i (WTW GmbH, Weilheim, Germany). In addition, turbidity [NTU] was assessed using a WTW® Turb 355 IR measuring set. Water depth [m] and near-bed flow velocity [$m \cdot s^{-1}$] were measured the next day using a magnetic inductive flow meter (Ott MF pro, Ott, Kempten, Germany). Flow velocity was directly measured at each spot 5 cm below the water surface and 3–5 cm above the substratum surface. To calibrate for potential surface roughness-induced bias through variability of emissivity (Handcock et al., 2012), we acquired point data of surface flow velocity and water surface roughness for each spot measurement and for each flight. The surface-roughness device was made out of a floating ball (80 mm diameter Styrofoam, Hagebaumarkt, Freising, Germany) on a lever-pointer arm, which transfers the movements of the water surface, directly on a display of a scale (Fig. S1). The lever-pointer arms are both 27 cm long to ensure 1:1 leverage ratio. Wave frequency within 30 s and the reading of the

minimum and maximum wave amplitude was recorded. Water surface roughness and surface flow velocity data were used for further analysis regarding thermal emissivity linked to fluvial thermal regions. Surface flow velocity was measured using peanut puffs floating on the surface between a defined distance of one meter and counting the time. Solar radiation was measured by means of nine additional UA-002-064 HOBO® loggers, which also measure radiation in Lux at the respective locations of physico-chemical point data collection. Solar radiation in Lux was converted to Watts per square meter [$W{\cdot}m^2$] using an approximate conversion of 0.0079 W/m^2 per Lux (Nouman et al., 2019).

2.3. Data analysis

To visualise thermal and physical habitat differences in thermal regions (Danube, OHB, LMB, CON, FP, BB), a non-metric multidimensional scaling (NMDS) analysis using PRIMER v7 (Plymouth Marine Laboratory, Plymouth, UK) was plotted. For this multivariate analysis, a resemblance matrix was calculated based on Euclidean distances (Clarke, 1993) using the complete data set of measured habitat variables across all individual flights (Clarke et al., 2014). To test for significant differences between thermal regions, a one-way analysis of similarities (ANOSIM, Clarke et al., 2014) based on the same resemblance matrix as for the NMDS, using Euclidean distances as described above, was used. To identify which of the abiotic variables fitted best with the ordination of thermal regions in the NMDS plot, a distance-based linear modelling (DistLM, Clarke et al., 2014) was performed using Primer v7 variables that were selected by DistLM as the best fit were displayed in the NMDS using the overlay function in PRIMER. For multivariate statistical tests, a significance level of $p < 0.05$ was applied.

To assess the complexity of thermal heterogeneity and its driving factors we applied several GLMMs. In order to account for the different spatial resolution of temperature data (pixel scale data derived from hourly drone flights) and the measured point data (measured simultaneously to the flights at spot measurements) we created a sub-dataset for calculating the GLMMs. In this sub-dataset we used temperature data on pixel basis in a three meter radius of our spot measurements in all thermal regions resulting in 9 sites that were assessed in the GLMMs (equates to the spot measurements indicated in Fig. 1). The following response variables (temperature metrics) were considered: median temperature, 5 % quantile of temperature values, 95 % quantile of temperature values, the standard deviation ±SD and the Shannon diversity (SH) of temperatures. We compared the response variables to the field-measured predictor variables through several general linear mixed effect models (GLMMs) performed in R (R packages car and tidyverse). The response variable median temperatures was selected to represent the central stream temperature values of the thermal region. The 5 % quantile and 95 % quantile were used to represent extreme temperature values. The ±SD and the Shannon diversity were used to represent the complex thermal heterogeneity in spatially resolved surface water temperatures. To allow for comparisons of the relative strength of predictor variables on temperature metrics, those data were normalised by subtracting the arithmetic mean and dividing by the standard deviation. In addition, predictor variables were tested for multi-collinearity using the Pearson method (Boslaugh and Watters, 2008). Only variables that revealed values <0.7 by the Pearson method were considered in the GLMMs (Nettleton, 2014). Subsequently, a total of 18 predictor variables were stepwise considered in the model for predicting temperature metrics. They included dissolved oxygen (O_2), turbidity (TB), pH-value (pH), electric conductivity (EC), water depth (D), diversity of water depths (DD), current speed (v), diversity of current speeds (Dv), macrophytes coverage (M), overhanging vegetation (OV), shaded area of water surface (SHD), solar radiation (SW), air temperature over water surface (AS), exposure of thermal region (EX), wind speed (WS), relative humidity (RH), surface roughness frequency (SR) and surface roughness amplitude (SA) (Table 1). To account for site variability and potential spatial autocorrelation between thermal regions and time of day, site and flight number (corresponding to daytime) were included as random effects. To consider potential interactions between variables relevant pairs were integrated in the model stepwise using the interaction term. Model selection followed the top-down strategy (Diggle et al., 2002) as described in Zuur et al. (2009). The Akaike Information Criteria (AIC) based on the restricted maximum likelihood (REML) was chosen as model selection tool for each of the five response variables. The *p*-values for predictor variables of the best-fitting model were obtained by Wald Chi-square tests. Significance was accepted at multiple levels $p < 0.10$ (.), $p < 0.05$ (*), $p < 0.01$ (**) and $p < 0.001$ (***).

Table 1
Factors considered in the GLMM and their Abbreviations used throughout the text.

Predictor variables	Abbreviation	Unit
Dissolved oxygen	O_2	$mg{\cdot}L^{-1}$
Turbidity	TB	NTU
pH-value	pH	pH
Electric conductivity	EC	$\mu S{\cdot}cm^{-1}$
Water depth	D	m
Diversity of water depths	DD	Shannon
Current speed	v	$m{\cdot}s^{-1}$
Diversity of current speeds	Dv	Shannon
Macrophyte coverage	M	%
Overhanging vegetation	OV	%
Shaded area of water surface	SHD	%
Solar radiation	SW	W/m^2
Air temperature over the surface	AS	°C
Exposure of thermal region	EX	E/W/S/N
Wind speed	WS	$m{\cdot}s^{-1}$
Relative humidity	RH	%
Surface roughness frequency	SR	Number of deflections
Surface roughness amplitude	SA	Span of values

To assess how temperatures can change over river length and time, a generalised additive model (GAM, see also Parmentier et al., 2015 and Laanaya et al., 2017) was used to consider stream surface temperatures of the OHB. Since the OHB was the only thermal region comprising a pronounced change in steepness along its course, we computed a generalised additive model (GAM) outside the GLMMs for a closer inspection of the interrelation between steepness and temperature changes for this case. We calculated a three-dimensional model of OHB mean temperature by variables distance to source and time, using Arcmap to create indexed polygon transects ($n = 66$, in 5 m distance) along the OHBs river centre line (overall length of the assessed river was 330 m) and intersected those polygons with a polygonised TIR-Image of each flight (daytime 6:00 to 20:00) of the OHB. To visualise changes in mean temperature by distance to source (Danube) and time of the day for the OHB, we applied a GAM using the function 'gam' in the R-package 'mgcv' (Wood, 2011). We calculated the mean temperature for each transect and assigned the transect index to the distance to the source (river Danube). GAM of response variable mean temperature was set up with variables distance to source and daytime (flight number) having a full tensor product smooth and interaction of time of the day and distance having a tensor product interaction. We used the r-package 'plotly' to present the model as a 3-dimensional surface plot.

3. Results

3.1. Spatio-temporal thermal habitat heterogeneity

The study area revealed both an expected daily thermal distribution and a large temperature heterogeneity across the assessed thermal regions in the aquatic habitats of the restored floodplain. The relatively low water temperatures in the morning warmed up during the course of the day and cooled down again towards the evening (Fig. 2 and Fig. 3). Depending on thermal region, an overall delay in the warming up of stream water of up to two hours compared to the increase in air temperatures was evident. In addition, some of the assessed thermal regions

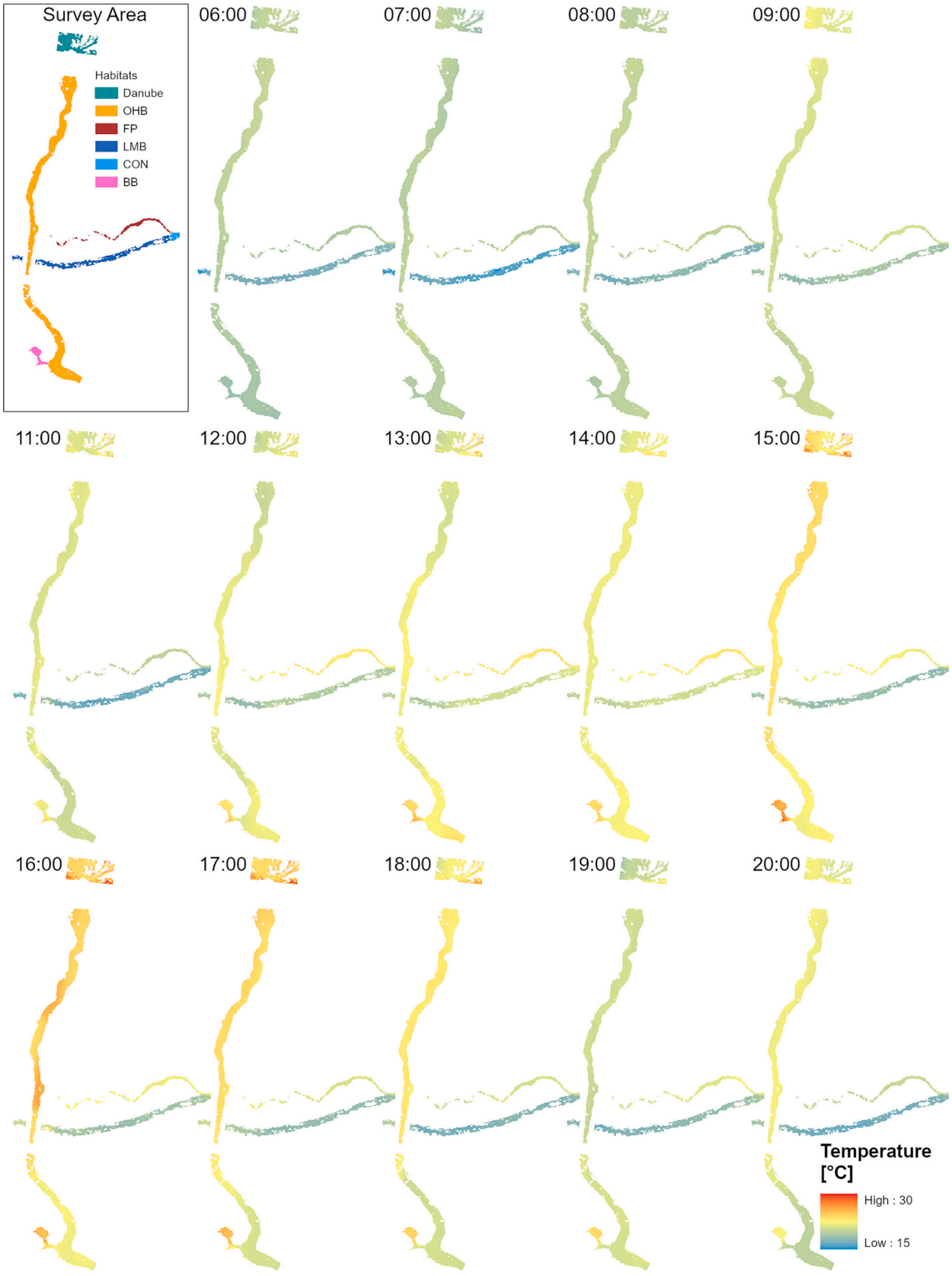

Fig. 2. Map of the study area including all assessed thermal regions and hourly flights during the day.

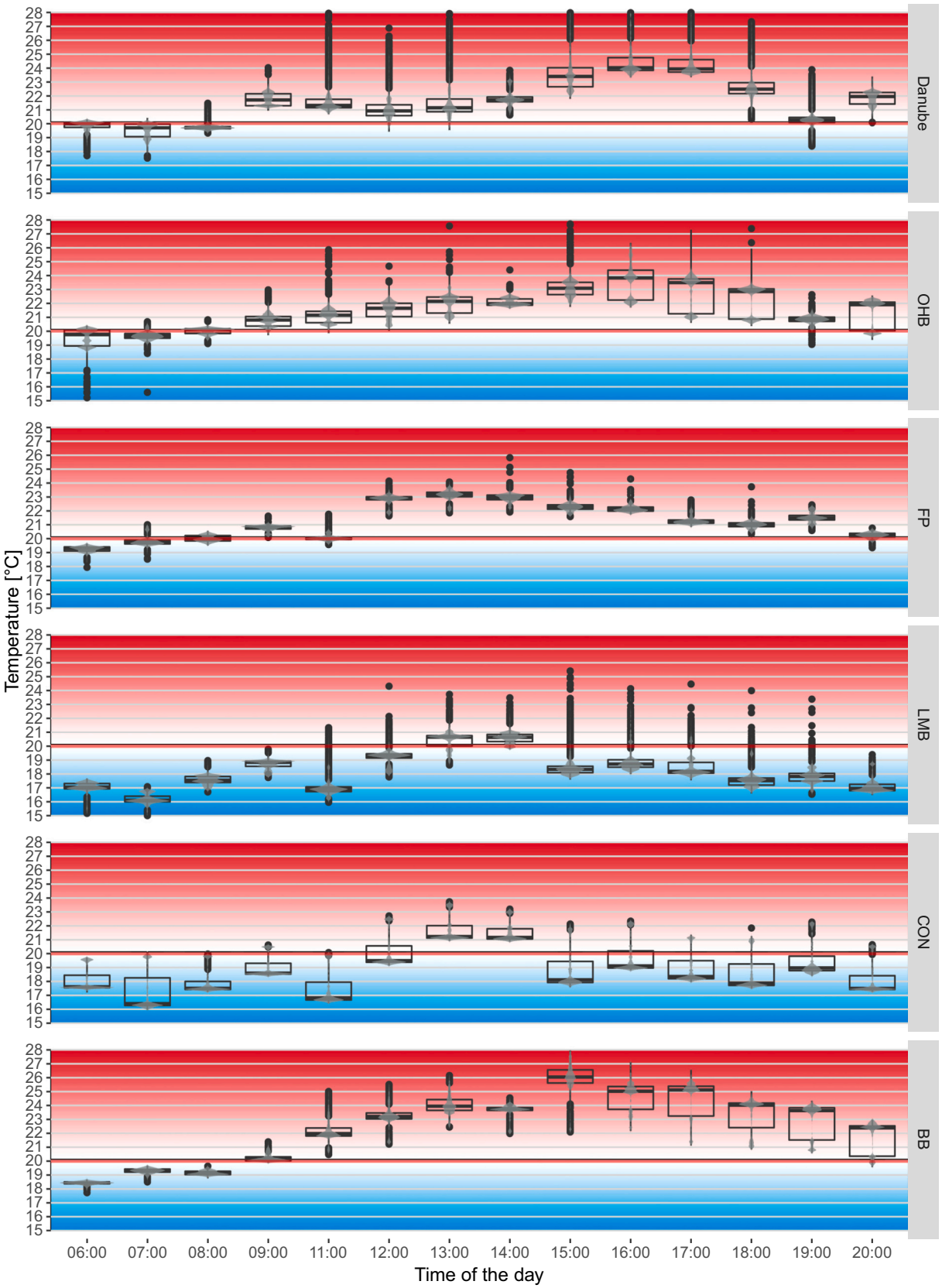

Fig. 3. Box-whisker-plot (25 % quantile, median, 75 % quantile, whisker: minimum and maximum values, circles represent outliers) of the diurnal temperatures derived from the hourly flights. In order to highlight temperature thresholds being known as upper limits for cold-water fish species such as salmonids (reviewed in Smialek et al., 2021), we designated a 20 °C threshold (known as a limit for brown trout) in the graph using indicative colours red (hot) and blue (cold) separated by a red line. The percentages above the plot indicate the proportion of pixels that have exceeded 20C° for each of the boxes.

presented different mean temperatures and warming patterns, with FP, LMB and CON peaking at the earliest hour (13.00 h), and Danube as well as OHB at 16:00 h.

In the thermal landscape, overall range of temperatures of aquatic habitats was larger than expected and ranged between 14.2 and 28.0 °C (mean = 20,7 °C), with peak median temperatures (26,1 °C) around 16:00 h (Fig. 3). After this time point, the thermal regions started to cool down, however, at 20:00 h they were still >2 °C warmer than in the first flight at 6:00 h in the morning. Highest temperatures were measured between 11:00 and 17:00 h (peaking around 28 °C in BB, Danube and OHB), while lowest temperatures of around 15 °C were only measured in the early morning until 7:00 h (in LMB and OHB) (Fig. 4).

During the day, the temperature regime in the thermal regions followed individual patterns, with different minimum, maximum and median temperatures. The groundwater influenced LMB and CON were the coolest regions, with temperatures during most of the day below 20 °C, except between 12:00 and 13:00 h. Warmest stream temperatures were found in the Danube, OHB, FP and BB only comprising temperatures below 20 °C in the early morning hours (Fig. 4). Highest temperature variation in thermal regions occurred between 11:00 and 18:00 h in the Danube, LMB and OHB, whereas lowest temperature variation occurred in the FP and the CON. The temperature pattern in the BB thermal region was most unique, with steadily increasing temperatures peaking at 15:00 h (Fig. 4).

Observed temperature differences in timing and amplitude among thermal regions were unexpectedly high and created a large temperature heterogeneity across the floodplain. For example, at the groundwater influenced LMB (mean temperature 18.24 °C, lowest temperature 15.00 °C, Fig. 5), several CWP (below 19.0 °C) were detected around 12:00 h, whilst other habitats such as the BB passed 21.0 °C (median 23 °C) at this time point (Fig. 4). Since the thermal region CON (mean 19.08 °C, Fig. 5) represents the confluence between the FP and LMB, it was also strongly influenced by the cooler groundwater of the LMB. The OHB (mean 21.38 °C) and subsequently the FP (mean 21.23 °C) are fed by Danube surface water (mean 21.59 °C) and were closely linked to the Danube's high temperatures (maximum 28.00 °C). According to the results of the GAM, the OHB was cooling down on its way through the floodplain (Fig. 2 and Fig. 6). The dropping temperatures corresponded to the steepness of the river along its assessed 330 m flow course and cooled down by about 2.25 °C over this stretch at 16:00 h (Fig. 6). Besides the Danube, highest (maximum 28.00 °C) and mean temperatures (22.33 °C) were detected in BB that is connected to the OHB.

Multivariate analysis, considering point data and imagery-extracted temperature data, by ANOSIM revealed significant differences between the assessed thermal regions displayed in the NMDS (Fig. 7, Table 2). DistLM ($R = 0.85$) identified as significantly best fitting variables to the NMDS instream variables (e.g. O_2, pH, EC, DD, SR, M, Dv, D, v, TB); as well as subsurface variables (e.g. AS, SW, RH, SHD, OV, SA, WS, EX). Assessing differences between thermal regions solely using temperature-related metrics such as median temperature, 5 % quantile and 95 % quantile, ±SD and Shannon diversity of temperature, multivariate analysis using ANOSIM become not significant between the thermal regions Danube – FP and OHB – FP (Table 2).

3.2. Drivers of spatial and temporal thermal heterogeneity

According to the calculated GLMMs, number and type of variables driving spatial and temporal temperature patterns changed with the complexity of temperature metrics used for the assessment. The number of variables which the model suggested as best fit (according to the lowest AIC) increased with increasing complexity of the temperature metrics used as response variables, e.g. Shannon diversity and ± SD. For Shannon diversity and ± SD, most variables (eight variables SH and seven ±SD, Table 3) were detected to contribute significantly to the model. Strongest correlations of predictor variables for the temperature metrics SD and SH were detected for OV, DV, EX, M and SHD. For the 95 % quantile of temperature data, seven variables (v was not significant), for the 5 % quantile five variables and for the median four variables were detected. In all of these three models, O_2, DD and M were identified as strongest predictors (highest correlation) for temperature. All five models identified the presence of M and SW as variables driving patterns in the temperature landscape. The DD was identified four times, and D and O_2 as an indicator for groundwater influence, three times. All other variables were only significant twice (v, Dv, OV and SHD) or once (TB, pH, EC and EX). Similar to the identified variables, the interactions in the model changed with increasing complexity of the response variables (Table 3). Interactions between O_2 and M were consistently highly significant across all levels of model complexity. The interaction of OV and SHD was significant three times, and the one between SW and AS two times. The interactions of SW and SHD, D and DD, as well as v and Dv were only detected once. In all models, the random effects site and flight number (flight no.) improved model performance.

4. Discussion

The findings of this study illustrate that stream thermal heterogeneity can be highly dynamic and spatially patchy across the riverscape. This heterogeneity and the connection between thermally different areas are currently hardly considered in the management of such systems, yet essential for assessing habitat suitability for target species of

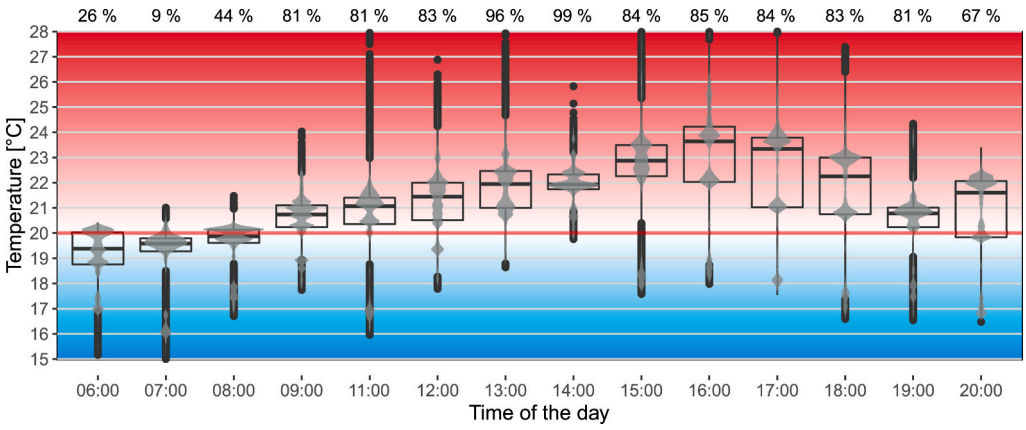

Fig. 4. Box-whisker-plot (25 % quantile, median, 75 % quantile, whisker: minimum and maximum values, circles represent outliers) of the diurnal temperature regime displayed for all flights and thermal regions separately. In order to highlight temperature thresholds being known as upper limits for cold-water fish species such as salmonids (reviewed in Smialek et al., 2021), we designated a 20 °C threshold (known as a limit for brown trout) in the graphs using indicative colours red (hot) and blue (cold) separated by a red line.

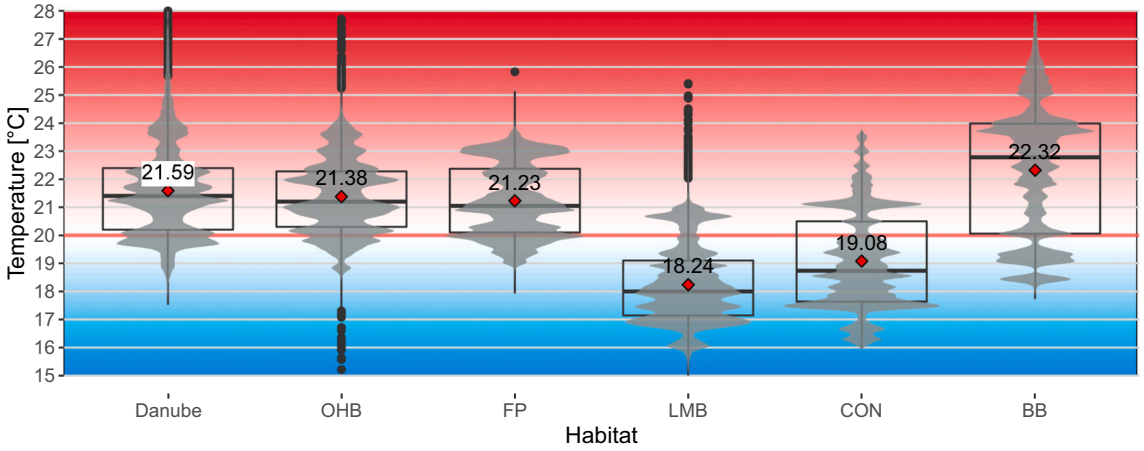

Fig. 5. Box-whisker-plot (25 % quantile, median, 75 % quantile, whisker: minimum and maximum values, circles represent outliers) of the general temperature patterns with pooled data of the sampling day. Red rough is indicating mean temperatures. In order to highlight temperature thresholds being known as upper limits for cold-water fish species such as salmonids (reviewed in Smialek et al., 2021), we designated a 20 °C threshold (known as a limit for brown trout) in the graphs using indicative colours red (hot) and blue (cold) separated by a red line.

conservation. The Danube floodplain restoration site reflected an unexpectedly strong warming and cooling cycle during a summer day, with distinctive thermal patterns in each differentiated thermal region, illustrating the complex mosaic of physical habitats. However, the temperature patterns in the thermal regions reflected not only the given structural aquatic habitat mosaic, but their dependence on several other factors such as groundwater input or solar radiation driving instream and subsurface processes.

4.1. Stream thermal heterogeneity

Recent studies have shown that many fish species that rely on cold-water conditions are declining (e.g. Lund et al., 2018; Mueller et al., 2020), and the situation may get worse under future climate change scenarios. Even slight changes of climate-related variables such as fine sediment input, temperature and flow have been shown to act synergistically (White et al., 2023), sometimes resulting in a complete die-off of the eggs of cold-water fish such as Danube salmon (Wild et al., 2023), brown trout (Casas-Mulet et al., 2021) and Atlantic salmon (Casas-Mulet et al., 2015). Suitable habitats for cold-water fish are, in principle, available across the study area. During our survey, however, water temperatures reached 28 °C, which clearly exceeds the tolerance limit for many salmonid species (Sullivan et al., 2000; Smialek et al., 2021). Some thermal regions, including Danube, BB, OHB and FP, were only suitable for cold water-adapted species in the morning hours until 9:00 am. After that time point, water temperatures rose above 20 °C, which is known to be a critical temperature exceeding optimal living conditions for salmonids (reviewed in Smialek et al., 2021). Cold water-adapted species may then be forced to move out of these rapidly warming habitats and seek CWPs elsewhere across the floodplain, making them heavily dependent on the connectivity between available habitats. However, rising mean water temperatures will undoubtedly lead to a scarcity of CWPs, increasing the distance between such cool areas (Kuhn et al., 2021), and forcing organisms to move further in their search for potential CWRs. Extreme temperatures may affect adult aquatic organisms and severely threaten critical life stages (e.g. Smith et al., 1975). For instance, BB-habitats are well known to be favoured by early life stages of fishes and later juvenile stages (Pander et al., 2021). When temperatures increase during the course of the day, it is very important that such habitats are fully connected to CWPs along the riverscape, otherwise it may lead to shifts or shortages in feeding hours for cold-stenothermic fish species. In the other thermal regions of the floodplain, such as the LMB or the CON, water temperatures were generally lower than in the Danube or the OHB, providing suitable habitats most of the day, except for the time between 13:00 and 14:00 h. During this time, cold-water-adapted species solely depend on CWPs inside these thermal regions since mean temperatures are much higher than tolerated maxima. It is thus important to inform river restoration management that connectivity of aquatic habitats is not only key to overcome riverine obstacles such as dams and hydropower plants in the context of fish spawning migration (Noonan et al., 2012), or to improve river morphology and structural habitat quality as done in classical river restoration approaches (Castro and Thorne, 2019; Cluer and Thorne, 2014; Wohl et al., 2021). Instead, it is also important to fully connect the mosaics of differentiated thermal regions and their CWPs across riverscapes (Casas-Mulet et al., 2020; Kuhn et al., 2021), and to consider the influence of land use in riparian strips and entire catchments on stream thermal profiles (Drainas et al., 2023).

In the study area at the Danube, a complex mosaic of morphologically different habitat types evolved after the floodplain restoration in the year 2010, resulting in a high species diversity (Pander et al., 2018). Past studies could only partly explain species occurrence patterns by exclusively considering structural properties of different habitat types within the floodplain. Adding the information on spatio-temporal temperature ranges and heterogeneities within this system can obviously explain the absence of cold-stenothermic species from some structurally suitable habitats such as river stretches (OHB) on the one hand, and the local dominance of cyprinids in warmer areas such as the BB. This dynamic spatio-temporal mosaic of cold and warm areas may have several advantages for aquatic species in the floodplain (Armstrong et al., 2021). In addition, for those species that can easily move between habitats, a switch between warm (faster growth) and cold (refuges) may be particularly advantageous. This underscores the need for a dynamic view of habitat functionality in riverscapes which simultaneously considers structural habitat and thermal dynamics including the relatively quick changes of living conditions for aquatic species (Thorp et al., 2006; Wohl, 2016). Such dynamics create the need to consider longitudinal, lateral, vertical and temporal connectivity as a highly complex requirement for river restoration (Powers et al., 2019; Weber et al., 2017; Wohl et al., 2021).

4.2. Drivers of spatial and temporal thermal heterogeneity

Only with a clear understanding of the processes driving stream thermal heterogeneity and CWPs, effective river restoration strategies can be implemented (Skidmore and Wheaton, 2022; Dugdale et al., 2013; Casas-Mulet et al., 2020). Within the morphological complexity of our restored floodplain, we identified groundwater influence, shading

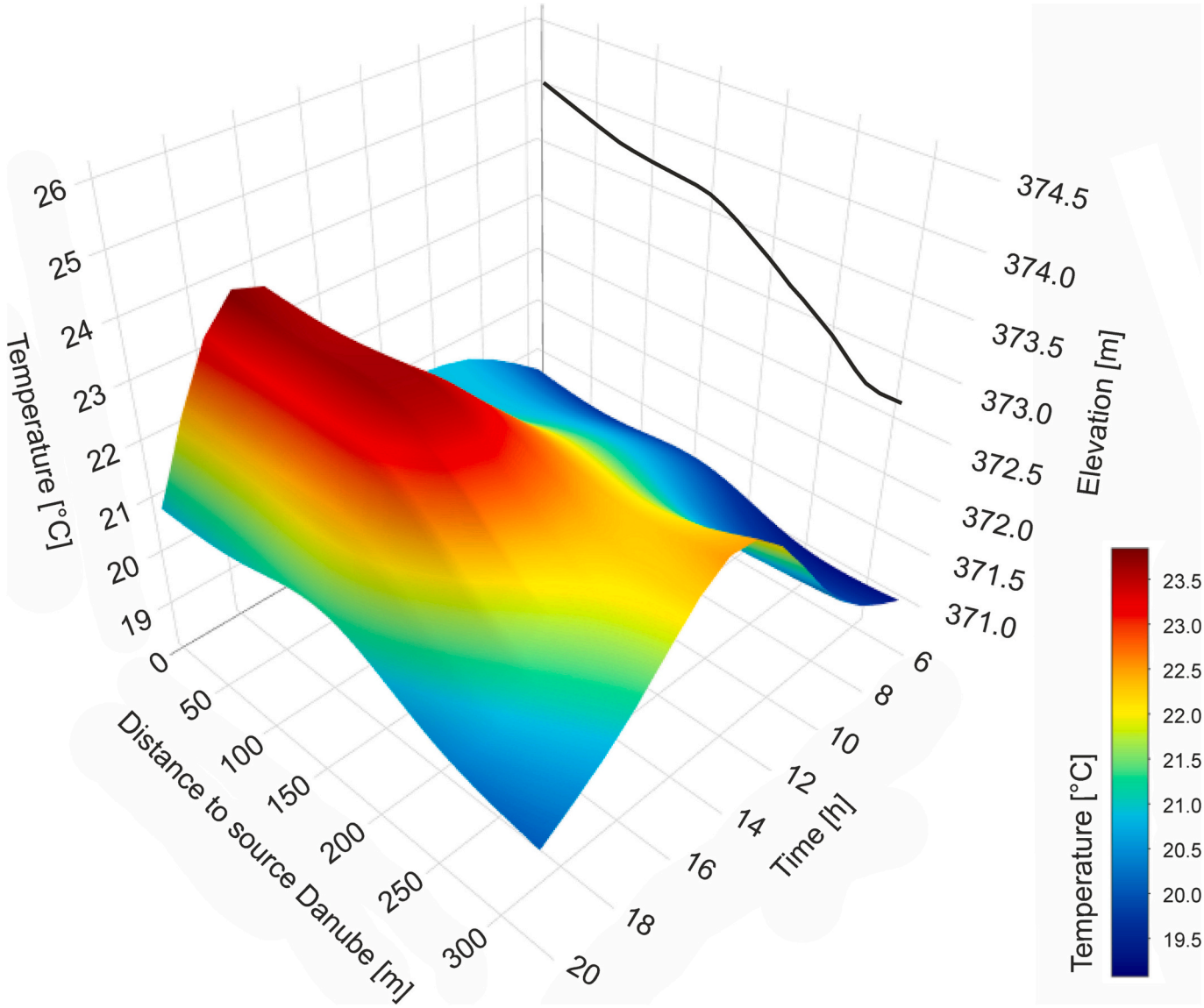

Fig. 6. Generalised additive model (GAM), with mean surface water temperatures of the Ottheinrichbach in relation to daytime, elevation and distance to the source Danube.

and river morphology as the key processes driving thermal riverscape heterogeneity. This is also in line with findings from other authors (e.g. Broadmeadow et al., 2011; Casas-Mulet et al., 2020; Dugdale et al., 2013; Drainas et al., 2023; Ebersole et al., 2003; Kalny et al., 2017), with a particular highlight on the links between fluvial geomorphology and hyporheic flows on stream temperatures (Burkholder et al., 2008; Arrigoni et al., 2008). On that note, the availability of O_2 and EC are well-known abiotic indicators of upwelling groundwater (Hayashi et al., 2012), which was particularly dominant in the LMB thermal region together with high macrophytes proliferation due to its clear water. In this context, also water-mixing zones between rivers are very important. The CON as mixing zone between LMB and FP comprised a unique temperature pattern (see Fig. 4 and Fig. 5) that likely depended on the mixing ratio of warm FP water and cold upwelling groundwater of the LMB. In the mixing zone, we detected a quick and turbulent intermix of both waters and the negative low oxygen levels of the groundwater influenced LMB get largely buffered by the rich oxygenated FP-water. This potentially promotes CWRs for cold-water fishes during the hottest times of the day, the latter also requiring high oxygenated waters. Shaded areas on the water surface and overhanging vegetation significantly influenced the models. In our case, those factors were strongly linked to surface emissivity and air temperature over the surface, highlighting the well-established knowledge on the importance of dense riparian vegetation to offset the warming of the water surface via local shading (e.g. Broadmeadow et al., 2011; Johnson, 2004), but also considering that the river's orientation can largely influence shading in relation to the course of the sun (Casas-Mulet et al., 2020), particularly in medium to large-size rivers. However, in our models, exposure of the thermal region was not detected as a significant factor, potentially due to the relative small size of our rivers indicating that local shading was more important. Such findings highlight the importance of riparian vegetation management as an easy, cost effective and powerful river restoration tool to mitigate river warming locally (Malcolm et al., 2004; Garner et al., 2015). In line with the findings above, hydromorphological factors such as depth diversity or current diversity were also detected by the models to be important drivers of CWPs underpinning the importance of these measures as a means to create thermal heterogeneity across the riverscape. Within the study region, the diversity of depth and current promoted fast flowing and cooler river sections with higher groundwater input (Evans and Petts, 1997) that in turn potentially increased the availability of CWPs (Kuhn et al., 2021). In our dataset, meteorological factors such as wind speed, air

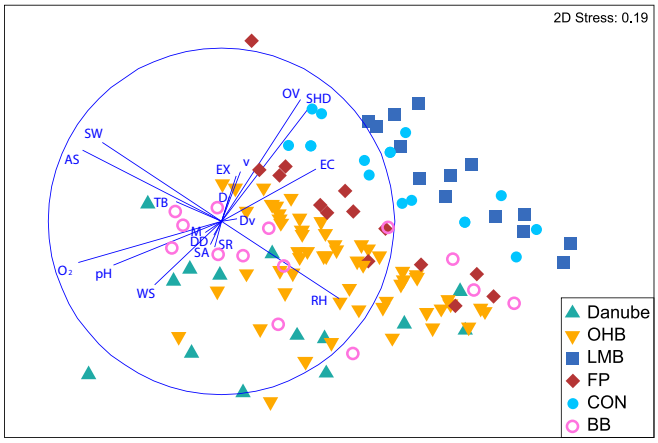

Fig. 7. NMDs displaying the structural, chemical and temperature dissimilarity between the assessed thermal regions based on Euclidean distance measures considering all measured habitat variables. Note that the NMDS only displays variables that were detected by DISTLM as best fit to the ordination of thermal regions. Abbreviations of the thermal landscape: OHB = Ottheinrichbach, LMB = Längenmühlbach, FP = fish pass, CON = confluence between OHB and LMB, BB = billabong. Abbreviations of habitat variables: O_2 = dissolved oxygen, pH = pH-value, EC = electric conductivity, TB = turbidity, v = current speed, Dv = diversity of current speed, D = depth, DD = diversity of depth, AS = air temperature at water surface, SW = solar radiation, EX = exposure, RH = relative humidity, SR = surface roughness, SA = surface roughness amplitude, M = macrophyte coverage, WS = wind speed, SHD = shaded area, OV = vegetation coverage.

temperature and relative humidity did not differ largely enough across the scale of thermal regions to be detected by the models as influencing factors.

4.3. Steepness as a driver of cooler water

The OHB temperature regime is largely driven by the Danube surface water at the origin and cools down the greater the steepness of the OHB gets along its flow course. Particularly as the slope of the OHB in the downstream third of the assessed river stretch increased, the surface water temperature cooled down successively about 2.5 °C. The observation that steeper reaches exhibit cooling is likely driven by the increased hydraulic head present in a steeper reach, increasing hyporheic exchange. This is also in line with the findings of Evans and Petts (1997) who found that water temperatures at the downstream end of steeper riffle sections can be lower due to a higher mixing rate of surface and interstitial water. In this context, a highly porous interstitial with coarse substratum as it is typical for riffle sections may favour hyporheic exchange. Potential mechanisms for the observation of cooling over steeper reaches beyond hyporheic engagement would be evaporative cooling from the addition of energy at the air-water interface. In our dataset, this was only the case in the early morning (before 8:00 a.m.). The disrupted/chaotic flow paths of a cascading surface can then drive phase change events - and, if the air temperature is cooler than the water, increased advective exchange due to the increased relative velocity gradients across the air-water interface (Evans and Petts, 1997). In combination with findings of Garner et al. (2017) who detected that shading can largely reduce solar radiation and can prevent small rivers from heating up during sunny days, restoration managers can use a combination of both tools to mitigate warming effects. This holds particularly true for heavily modified rivers such as the upper Danube, where a reset of the riverscape to the "stage zero" (Bowles et al., 2021; Powers et al., 2019) is not possible, yet the construction of side channels with steep sections and riparian vegetation providing shading is a feasible option. Whilst reach-scale topographic gradients cannot be easily changed, restoration can still target the micro-habitat scale

Table 2
Results of the multivariate comparisons by ANOSIM of the different assessed thermal regions in the restored Danube floodplain. All variables = measured point data as well as spatial thermal data from the UAS flights of the thermal regions (OHB = Ottheinrichbach, LMB = Längenmühlbach, FP = fish pass, CON = confluence between OHB and LMB, BB = billabong and Danube) are considered. Temperature metrics = solely considers spatial thermal data from the UAS flights of the thermal regions. R = ratio between within-group and between-group dissimilarities. The closer this value is to one, the more the sites within a group are similar to each other and dissimilar to sites in other groups. Significance of results was accepted at $p < 0.05$.

			R	*p*-Value
All variables	Global test		0.611	<0.001
	Differences between thermal regions	Danube - OHB	0.662	<0.001
		Danube - LMB	0.806	<0.001
		Danube - FP	0.697	<0.001
		Danube - CON	0.730	<0.001
		Danube - BB	0.322	<0.001
		OHB - LMB	0.708	<0.001
		OHB - FP	0.345	<0.001
		OHB - CON	0.664	<0.001
		OHB - BB	0.529	<0.001
		LMB - FP	0.823	<0.001
		LMB - CON	0.788	<0.001
		LMB - BB	0.755	<0.001
		FP - CON	0.628	<0.001
		FP - BB	0.529	<0.001
		CON - BB	0.662	<0.001
Temperature metrics	Global test		0.382	<0.001
	Differences between thermal regions	Danube - OHB	0.164	<0.01
		Danube - LMB	0.728	<0.001
		Danube - FP	0.014	>0.05
		Danube - CON	0.417	<0.001
		Danube - BB	0.131	<0.05
		OHB - LMB	0.642	<0.001
		OHB - FP	0.011	>0.05
		OHB - CON	0.549	<0.001
		OHB - BB	0.333	<0.001
		LMB - FP	0.676	<0.001
		LMB - CON	0.585	<0.001
		LMB - BB	0.608	<0.001
		FP - CON	0.480	<0.001
		FP - BB	0.129	<0.05
		CON - BB	0.526	<0.001

vertical topographical roughness. This is particularly the case in highly regulated rivers where damming often results in much higher than the natural water levels of the river in the upstream sections of dams (Mueller et al., 2011). If in addition, the four-dimensional connectivity as basis for successful colonisation is fulfilled, it can promote the idea of biomic river restoration (Johnson et al., 2020) likely leading to higher ecological functionality of biological processes in these systems as well.

Overall our study reflects that a more complex understanding of the four dimensions of habitat connectivity (lateral, longitudinal, vertical and during the day) is needed and should be transferred into effective river restoration measures to mitigate climate change induced river warming and support freshwater ecosystem resilience. It provides the basis to understand how daily changes in stream temperatures potentially affect ecological processes, using the thermal requirements of keystone species discussed herein as an example for cold stenothermic salmonids. In this context, the study identifies priority areas and potential types of restoration measures (e.g. creating side channels,

Table 3
Statistical output of the best fitting general linear mixed effects models (GLMMs). Models were calculated for the response variables: median temperature (Median), 5 % quantile of temperature values (5 % Q), 95 % quantile of temperature values (95 % Q), the standard deviation (±SD) and the Shannon diversity (SH) of temperatures values. Predictor variables: dissolved oxygen = O_2, turbidity = TB, pH-value = pH, electric conductivity = EC, water depth = D, diversity of water depths = DD, current speed = v, diversity of current speeds = Dv, macrophyte coverage = M, overhanging vegetation = OV, shaded area of water surface = SHD, solar radiation = SW, air temperature over the surface = AS, exposure of thermal region = EX, wind speed = WS, relative humidity = RH, surface roughness frequency = SR, surface roughness amplitude = SA. Yes = detected in the specific model, no = not detected in the specific model. Asterisk and dot indicate level of significance: .<0.1, * < 0.05, ** < 0.01, *** < 0.001. Site corresponds to the spot measurements given in Fig. 1 and flight no. corresponds to the time of the day. AIC = Akaike information criterion. Note that O_2 percentage, SR minimum and SR maximum values, Water temperature measured with the handheld device, air temperature at the spot measurements, daytime, cross wind, head wind and solar radiation measured in lux were excluded from the analyses.

	Variable	Median	5 % Q	95 % Q	±SD	SH
Variables selected by GLMM	O_2	Yes***	Yes***	Yes***	No	No
	TB	No	No	No	No	Yes*
	pH	No	No	No	No	Yes***
	EC	No	No	Yes**	No	No
	D	No	No	Yes**	Yes***	Yes***
	DD	Yes**	Yes***	Yes**	Yes***	No
	v	No	Yes.	Yes	No	No
	Dv	No	No	No	Yes***	Yes***
	M	Yes***	Yes**	Yes*	Yes***	Yes***
	OV	No	No	No	Yes***	Yes***
	SHD	No	No	No	Yes**	Yes***
	EX	No	No	No	Yes***	No
	SW	Yes***	Yes***	Yes***	Yes	Yes*
Interactions	D:DD	No	No	No	No	Yes***
	O_2:M	Yes***	Yes***	Yes**	Yes***	Yes***
	SW:SHD	Yes	No	No	No	No
	v:Dv	No	Yes***	No	No	No
	SW:AS	No	No	No	Yes	Yes
	OV:SHD	Yes**	No	No	Yes***	Yes***
Random effects	Site	Yes	Yes	Yes	Yes	Yes
	Flight no.	Yes	Yes	Yes	Yes	Yes
AIC		331.29	346.91	316.81	−249.87	32.55

riparian vegetation planting, dead wood introduction and gravel substrate replenishment) that could be applied to mitigate climatic extremes, supporting freshwater conservation management. Furthermore, the reliability and efficiency of innovative remote sensing tools to assess freshwater habitat quality and suitability were tested revealing certain changing patterns in daily stream temperatures that can be extremely useful for river habitat surveys and the understanding how assessment outcomes may vary based on daytime they have been carried out.

5. Conclusion

Temperature heterogeneity in riverscapes is more than a reflectance of physical habitat heterogeneity and can be highly dynamic spatially and temporally as shown in this study during a warm summer day. Thereby the distribution of surface temperatures can be largely dependent on instream variables expressing upwelling groundwater as well as on the habitat mosaic of the land-water interface expressed in variables such as shading or surface air temperature. This heterogeneity and the connection between thermally different areas are currently hardly considered in managing such systems, yet essential for assessing habitat suitability. By testing the reliability and efficiency of innovative remote sensing tools for assessing freshwater habitat, this study provides the basis to understand diurnal changes in stream temperatures and their links to ecological processes. Since restoring thermal refuges for aquatic biota will get more and more relevant in a steadily warming environment, river restoration should consider both measures to physically prevent habitat from excessive warming and measures to improve connectivity that meet the temperature developments in mosaics of complex and dynamic temperature riverscapes.

Supplementary data to this article can be found online at https://doi.org/10.1016/j.scitotenv.2024.170786.

CRediT authorship contribution statement

Joachim Pander: Writing – original draft, Visualization, Methodology, Investigation, Funding acquisition, Formal analysis, Data curation, Conceptualization. **Johannes Kuhn:** Writing – original draft, Visualization, Methodology, Investigation, Formal analysis, Data curation, Conceptualization. **Roser Casas-Mulet:** Writing – original draft, Resources, Methodology, Investigation, Funding acquisition, Conceptualization. **Luis Habersetzer:** Writing – original draft, Visualization, Investigation, Data curation. **Juergen Geist:** Writing – review & editing, Validation, Supervision, Resources, Project administration, Investigation, Funding acquisition, Conceptualization.

Declaration of competing interest

The authors declare that they have no known competing financial interests or personal relationships that could have appeared to influence the work reported in this paper.

Data availability

Data will be made available on request.

Acknowledgements

We thank the Auen Zentrum Neuburg-Ingolstadt, in particular B. Cyffka, for coordination of the permissions needed from the landowners. We also would like to thank the water authorities, in particular B. Kuegel from the local water authority, for their kind support of the study. We are also grateful to all the volunteers and student assistants who helped to measure all the predictor variables in the field during the drone flights. This research was partly funded by the Alexander von Humboldt Foundation through a fellowship awarded to RC-M under supervision of JG at TUM. In addition, we thank the HIT-Umweltstiftung, particularly C. Heider, for financial support.

References

Armstrong, J.B., Schindler, D., 2013. Going with the flow: spatial distributions of juvenile Coho Salmon track an annually shifting mosaic of water temperature. Ecosystems 16, 1429–1441. https://doi.org/10.1007/s10021-013-9693-9.

Armstrong, J.B., Fullerton, A.H., Jordan, C.E., Ebersole, J.L., Bellmore, J.R., Arismendi, I., Penaluna, B.E., Reeves, G.H., 2021. The importance of warm habitat to the growth regime of cold-water fishes. Nat. Clim. Chang. 11, 354–361. https://doi.org/10.1038/s41558-021-00994-y.

Arrigoni, A.S., Poole, G.C., Mertes, L.A.K., O'Daniel, S.J., Woessner, W.W., Thomas, S.A., 2008. Buffered, lagged, or cooled? Disentangling hyporheic influences on temperature cycles in stream channels. Water Resour. Res. 44, 1–13. https://doi.org/10.1029/2007WR006480.

Bierschenk, A.M., Mueller, M., Pander, J., Geist, J., 2019. Impact of catchment land use on fish community composition in the headwater areas of Elbe, Danube and Main. Sci. Total Environ. 652, 66–74. https://doi.org/10.1016/j.scitotenv.2018.10.218.

Boslaugh, S., Watters, P.A., 2008. Statistics in a Nutshell: A Desktop Quick Reference, 2nd edition. O'Reilly Media, Sebastopol, CA, p. 571.

Bowles, F., Clarke, S., Eardley, B., Jeffries, R., Stone, P., 2021. The stage zero approach – lessons from North America on restoring river, wetland and floodplain habitats. Conservation Land Management 19 (4), 21–28.

Braun, A., Auerswald, K., Geist, J., 2012. Drivers and spatio-temporal extent of hyporheic patch variation: implications for sampling. PloS One 7, e42046. https://doi.org/10.1371/journal.pone.0042046.

Broadmeadow, S.B., Jones, J.G., Langford, T.E.L., Shaw, P.J., Nisbet, T.R., 2011. The influence of riparian shade on lowland stream water temperatures in southern England and their viability for brown trout. River Res. Appl. 27 (2), 226–237. The influence of riparian shade on lowland stream water temperatures in southern England and their viability for brown trout.

Brunke, M., Gonser, T.O.M., 1997. The ecological significance of exchange processes between rivers and groundwater. Freshwater Biology 37 (1), 1–33. https://doi.org/10.1046/j.1365-2427.1997.00143.x.

Burkholder, B.K., Grant, G.E., Haggerty, R., Khangaonkar, T., Wampler, P.J., 2008. Influence of hyporheic flow and geomorphology on temperature of a large, gravel-bed river, Clackamas River, Oregon, USA. Hydrological Processes: An International Journal 22 (7), 941–953. https://doi.org/10.1002/hyp.6984.

Caissie, D., 2006. The thermal regime of rivers: A review. Freshw. Biol. 51, 1389–1406. https://doi.org/10.1111/j.1365-2427.2006.01597.x.

Carbonneau, P., Fonstad, M.A., Marcus, W.A., Dugdale, S.J., 2012. Making riverscapes real. Geomorphology 137, 74–86. https://doi.org/10.1016/j.geomorph.2010.09.030.

Casas-Mulet, R., Alfredsen, K., Brabrand, Å., Saltveit, S.J., 2015. Survival of eggs of Atlantic salmon (*Salmo salar*) in a drawdown zone of a regulated river influenced by groundwater. Hydrobiologia 743 (1), 269–284. https://doi.org/10.1007/s10750-014-2043-x.

Casas-Mulet, R., Pander, J., Ryu, D., Stewardson, M.J., Geist, J., 2020. Unmanned aerial vehicle (UAV)-based thermal infra-red (TIR) and optical imagery reveals multi-spatial scale controls of cold-water areas over a groundwater-dominated Riverscape. Front. Environ. Sci. 8, 64. https://doi.org/10.3389/fenvs.2020.00064.

Casas-Mulet, R., Matthews, E., Geist, J., Durance, I., Cable, J., 2021. Negative effects of parasite exposure and variable thermal stress on brown trout (*Salmo trutta*) under future climatic and hydropower production scenarios. Climate Change Ecology 2, 100039. https://doi.org/10.1016/j.ecochg.2021.100039.

Castro, J.M., Thorne, C.R., 2019. The stream evolution triangle: integrating geology, hydrology, and biology. River Res. Appl. 35 (4), 315–326. https://doi.org/10.1002/rra.3421.

Clarke, K.R., 1993. Non-parametric multivariate analyses of changes in community structure. Aust. J. Ecol. 18, 117–143. https://doi.org/10.1111/j.1442-9993.1993.tb00438.x.

Clarke, K.R., Gorley, R.N., Somerfield, P.J., Warwick, R.M., 2014. Change in Marine Communities: An Approach to Statistical Analysis and Interpretation, 3rd ed. Plymouth, UK, PRIMER-E, p. 144.

Cluer, B., Thorne, C., 2014. A stream evolution model integrating habitat and ecosystem benefits. River Res. Appl. 30 (2), 135–154. https://doi.org/10.1002/rra.2631.

Dal Sasso, S.F., Pizarro, A., Manfreda, S., 2021. Recent advancements and perspectives in UAS-based image velocimetry. Drones 5 (3), 81. https://doi.org/10.3390/drones5030081.

Daniels, M.E., Danner, E.M., 2020. The drivers of river temperatures below a large dam. Water Resour. Res. 56 (5), e2019WR026751 https://doi.org/10.1029/2019WR026751.

Diggle, P.J., Heagerty, P.J., Liang, K.Y., Zeger, S.L., 2002. Analysis of Longitudinal Data, *2nd ed.* Oxford University Press, Oxford, England, p. 398.

Drainas, K., Kaule, L., Mohr, S., Uniyal, B., Wild, R., Geist, J., 2023. Predicting stream water temperature with artificial neural networks based on open-access data. Hydrol. Process. 37, e14991 https://doi.org/10.1002/hyp.14991.

Dugdale, S.J., 2016. A practitioner's guide to thermal infrared remote sensing of rivers and streams: recent advances, precautions and considerations. WIREs Wate 3, 251–268. https://doi.org/10.1002/wat2.1135.

Dugdale, S.J., Bergeron, N.E., St-Hilaire, A., 2013. Temporal variability of thermal refuges and water temperature patterns in an Atlantic salmon river. Remote Sens. Environ. 136, 358–373. https://doi.org/10.1016/J.RSE.2013.05.018.

Dugdale, S.J., Bergeron, N.E., St-Hilaire, A., 2015. Spatial distribution of thermal refuges analysed in relation to riverscape hydromorphology using airborne thermal infrared imagery. Remote Sens. Environ. 160, 43–55. https://doi.org/10.1016/J.RSE.2014.12.021.

Dugdale, S.J., Kelleher, C.A., Malcolm, I.A., Caldwell, S., Hannah, D.M., 2019. Assessing the potential of drone-based thermal infrared imagery for quantifying river temperature heterogeneity. Hydrol. Process. 33, 1152–1163. https://doi.org/10.1002/hyp.13395.

Ebersole, J.L., Liss, W.J., Frissell, C.A., 2003. Cold water patches in warm streams: physicochemical characteristics and the influence of shading. J. Am. Water Resour. Assoc. 39, 355–368. https://doi.org/10.1111/j.1752-1688.2003.tb04390.x.

Eschbach, D., Piasny, G., Schmitt, L., Pfister, L., Grussenmeyer, P., Koehl, M., Skupinski, G., Serradj, A., 2017. Thermal-infrared remote sensing of surface water–groundwater exchanges in a restored anastomosing channel (upper Rhine River, France). Hydrol. Process. 31 (5), 1113–1124. https://doi.org/10.1002/hyp.11100.

Evans, E.C., Petts, G.E., 1997. Hyporheic temperature patterns within riffles. Hydrol. Sci. J. 42 (2), 199–213. https://doi.org/10.1080/02626669709492020.

Fausch, K.D., Torgersen, C.E., Baxter, C.V., Li, H.W., 2002. Landscapes to riverscapes: bridging the gap between research and conservation of stream fishes. BioScience 52, 483–498. https://doi.org/10.1641/0006-3568(2002)052[0483:LTRBTG]2.0.CO;2.

Fullerton, A.H., Torgersen, C.E., Lawler, J.J., Steel, E.A., Ebersole, J.L., Lee, S.Y., 2018. Longitudinal thermal heterogeneity in rivers and refugia for Coldwater species: effects of scale and climate change. Aquat. Sci. 80, 1–15. https://doi.org/10.1007/s00027-017-0557-9.

Garner, G., Malcolm, I.A., Sadler, J.P., Millar, C.P., Hannah, D.M., 2015. Inter-annual variability in the effects of riparian woodland on micro-climate, energy exchanges and water temperature of an upland Scottish stream. Hydrol. Process. 29 (6), 1080–1095. https://doi.org/10.1002/hyp.10223.

Garner, G., Malcolm, I.A., Sadler, J.P., Hannah, D.M., 2017. The role of riparian vegetation density, channel orientation and water velocity in determining river temperature dynamics. J. Hydrol. 553, 471–485. https://doi.org/10.1016/j.jhydrol.2017.03.024.

Geist, J., 2015. Seven steps towards improving freshwater conservation. Aquatic Conservation Marine and Freshwater Ecosystems 25, 447–453. https://doi.org/10.1002/aqc.2576.

Geist, J., Hawkins, S.J., 2016. Habitat recovery and restoration in aquatic ecosystems: current progress and future challenges. Aquatic Conservation Marine and Freshwater Ecosystems 26, 942–962. https://doi.org/10.1002/aqc.2702.

Gilvear, D.J., Spray, C.J., Casas-Mulet, R., 2013. River rehabilitation for the delivery of multiple ecosystem services at the river network scale. J. Environ. Manage. 126, 30–43. https://doi.org/10.1016/j.jenvman.2013.03.026.

Handcock, R.N., Torgersen, C.E., Cherkauer, K.A., Gillespie, A.R., Tockner, K., Faux, R. N., Tan, J., 2012. Thermal infrared remote sensing of water temperature in riverine landscapes. In: Patrice E. Carbonneau und Hervé Piégay (Hg.). Fluvial Remote Sensing for Science and Management, Bd. 3753. Wiley, S, pp. 85–113. https://doi.org/10.1016/S0034-4257(01)00186-9.

Hayashi, M., Vogt, T., Mächler, L., Schirmer, M., 2012. Diurnal fluctuations of electrical conductivity in a pre-alpine river: effects of photosynthesis and groundwater exchange. J. Hydrol. 450, 93–104. https://doi.org/10.1016/j.jhydrol.2012.05.020.

Huang, Q., Zeng, Z., 2017. A review on real-time 3D ultrasound imaging technology. Biomed. Res. Int. 2017 https://doi.org/10.1155/2017/6027029.

Isaak, D.J., Young, M.K., Nagel, D.E., Horan, D.L., Groce, M.C., 2015. The cold-water climate shield: delineating refugia for preserving salmonid fishes through the 21st century. Glob. Chang. Biol. 21, 2540–2553. https://doi.org/10.1111/gcb.12879.

Johnson, S.L., 2004. Factors influencing stream temperatures in small streams: substrate effects and a shading experiment. Can. J. Fish. Aquat. Sci. 61 (6), 913–923. https://doi.org/10.1139/f04-040.

Johnson, M.F., Thorne, C.R., Castro, J.M., Kondolf, G.M., Mazzacano, C.S., Rood, S.B., Westbrook, C., 2020. Biomic river restoration: A new focus for river management. River Res. Appl. 36 (1), 3–12. https://doi.org/10.1002/rra.3529.

Kalny, G., Laaha, G., Melcher, A., Trimmel, H., Weihs, P., Rauch, H.P., 2017. The influence of riparian vegetation shading on water temperature during low flow conditions in a medium sized river. Knowledge & Management of Aquatic Ecosystems 418, 1–14. https://doi.org/10.1051/kmae/2016037.

Kaushal, S.S., Likens, G.E., Jaworski, N.A., Pace, M.L., Sides, A.M., Seekell, D., Belt, K.T., Secor, D.H., Wingate, R.L., 2010. Rising stream and river temperatures in the United States. Front. Ecol. Environ. 8, 461–466. https://doi.org/10.1890/090037.

Kaylor, M.J., Justice, C., Armstrong, J.B., Staton, B.A., Burns, L.A., Sedell, E., White, S. M., 2021. Temperature, emergence phenology and consumption drive seasonal shifts in fish growth and production across riverscapes. J. Anim. Ecol. 90 (7), 1727–1741. https://doi.org/10.1111/1365-2656.13491.

Keppel, G., Mokany, K., Wardell-Johnson, G.W., Phillips, B.L., Welbergen, J.A., Reside, A.E., 2015. The capacity of refugia for conservation planning under climate change. Front. Ecol. Environ. 13, 106–112. https://doi.org/10.1890/140055.

Kuhn, J., Casas-Mulet, R., Pander, J., Geist, J., 2021. Assessing stream thermal heterogeneity and cold-water patches from UAV-based imagery: A matter of classification methods and metrics. Remote Sens. (Basel) 13, 1379. https://doi.org/10.3390/rs13071379.

Kurylyk, B.L., Macquarrie, K.T.B., Linnansaari, T., Cunjak, R.A., Curry, R.A., 2015. Preserving, augmenting and creating cold-water thermal refugia in rivers: concepts derived from research on the Miramichi River. New Brunswick (Canada). https://doi.org/10.1002/eco.1566/abstract.

Laanaya, F., St-Hilaire, A., Gloaguen, E., 2017. Water temperature modelling: comparison between the generalized additive model, logistic, residuals regression and linear regression models. Hydrol. Sci. J. 62 (7), 1078–1093. https://doi.org/10.1080/02626667.2016.1246799.

Leclerc, C., Reynaud, N., Danis, P.A., Moatar, F., Daufresne, M., Argillier, C., Usseglio-Polatera, P., Vernaux, V., Dedieu, N., Sentis, A., 2023. Temperature, productivity, and habitat characteristics collectively drive lake food web structure. Glob. Chang. Biol. 29 (9), 2450–2465. https://doi.org/10.1111/gcb.16642.

Letcher, B.H., Hocking, D.J., O'Neil, K., Whiteley, A.R., Nislow, K.H., O'Donnell, M.J., 2016. A hierarchical model of daily stream temperature using air-water temperature synchronization, autocorrelation, and time lags. PeerJ 4, e1727. https://doi.org/10.7717/peerj.1727.

Leuner, E., Schubert, M., Klein, M., 2013. Die Situation des Europäischen Aals (*Anguilla anguilla*) in Bayern. Bayerische Landesanstalt für Landwirtschaft, Freising, Germany, p. 44.

Lund, J., Medellin-Azuara, J., Durand, J., Stone, K., 2018. Lessons from California's 2012–2016 drought. J. Water Resour. Plan. Manag. 144 (10), 04018067 https://doi.org/10.1061/(ASCE)WR.1943-5452.0000984.

Maes, W.H., Steppe, K., 2019. Perspectives for remote sensing with unmanned aerial vehicles in precision agriculture. Trends Plant Sci. 24 (2), 152–164. https://doi.org/10.1016/j.tplants.2018.11.007.

Malcolm, I.A., Hannah, D.M., Donaghy, M.J., Soulsby, C., Youngson, A.F., 2004. The influence of riparian woodland on the spatial and temporal variability of stream water temperatures in an upland salmon stream. Hydrol. Earth Syst. Sci. 8 (3), 449–459. https://doi.org/10.5194/hess-8-449-2004.

McCluney, K.E., Poff, N.L., Palmer, M.A., Thorp, J.H., Poole, G.C., Williams, B.S., Williams, M.R., Baron, J.S., 2014. Riverine macrosystems ecology: sensitivity, resistance, and resilience of whole river basins with human alterations. Front. Ecol. Environ. 48–58 https://doi.org/10.1890/120367.

Mejia, F.H., Ouellet, V., Briggs, M.A., Carlson, S.M., Casa-Mulet, R., Chapman, M., Collins, M.J., Dugdale, S.J., Ebersole, J.L., Frechette, D.M., Fullerton, A.H., Gillis, C.-A., Johnson, Z.C., Kelleher, C., Kurylyk, B.L., Lave, R., Letcher, B.H., Myrvold, K.M., Nadeau, T.-L., Neville, H., Piégay, H., Smith, K.A., Tonolla, D., Torgensen, C.E., 2023. Closing the gap between science and management of cold-water refuges in rivers and streams. Glob. Chang. Biol. 00, 1–27. https://doi.org/10.1111/gcb.16844.

Messina, S., Costantini, D., Eens, M., 2023. Impacts of rising temperatures and water acidification on the oxidative status and immune system of aquatic ectothermic vertebrates: A meta-analysis. Sci. Total Environ. 868, 161580 https://doi.org/10.1016/j.scitotenv.2023.161580.

Mishra, V., Avtar, R., Prathiba, A.P., Mishra, P.K., Tiwari, A., Sharma, S.K., Singh, C.H., Yadav, B.C., Jain, K., 2023. Uncrewed aerial systems in water resource management and monitoring: a review of sensors, applications, software, and issues. Advances in Civil Engineering 2023. https://doi.org/10.1155/2023/3544724.

Morelli, T.L., Daly, C., Dobrowski, S.Z., Dulen, D.M., Ebersole, J.L., Jackson, S.T., Lundquist, J.D., Millar, C.I., Maher, S.P., Monahan, W.B., Nydick, K.R., Redmond, K. T., Sawyer, S.C., Stock, S., Beissinger, S.R., 2016. Managing climate change refugia for climate adaptation. PloS One 11, e0159909. https://doi.org/10.1371/journal.pone.0159909.

Mueller, M., Pander, J., Geist, J., 2011. The effects of weirs on structural stream habitat and biological communities. J. Appl. Ecol. 48, 1450–1461. https://doi.org/10.1111/j.1365-2664.2011.02035.x.

Mueller, M., Bierschenk, A.M., Bierschenk, B.M., Pander, J., Geist, J., 2020. Effects of multiple stressors on the distribution of fish communities in 203 headwater streams of Rhine, Elbe and Danube. Sci. Total Environ. 703, 134523 https://doi.org/10.1016/j.scitotenv.2019.134523.

Nettleton, D., 2014. Commercial Data Mining. Processing, Analysis and Modeling for Predictive Analytics Projects. Elsevier, New York, USA, p. 287.

Noonan, M.J., Grant, J.W., Jackson, C.D., 2012. A quantitative assessment of fish passage efficiency. Fish Fish. 13 (4), 450–464. https://doi.org/10.1111/j.1467-2979.2011.00445.x.

Nouman, A.S., Chokhachian, A., Santucci, D., Auer, T., 2019. Prototyping of environmental kit for georeferenced transient outdoor comfort assessment. ISPRS Int. J. Geo Inf. 8 (2), 76. https://doi.org/10.3390/ijgi8020076.

Orr, H.G., Simpson, G.L., des Clers, S., Watts, G., Hughes, M., Hannaford, J., Dunbar, M. J., Laizé, C.L.R., Wilby, R.L., Battarbee, R.W., Evans, R., 2015. Detecting changing river temperatures in England and Wales. Hydrol. Process. 29, 752–766. https://doi.org/10.1002/hyp.10181.

Palmer, M.A., Reidy Liermann, C.A., Nilsson, C., Flörke, M., Alcamo, J., Lake, P.S., Bond, N., 2008. Climate change and the world's river basins: anticipating management options. Front. Ecol. Environ. 6, 81–89. https://doi.org/10.1890/060148.

Pander, J., Mueller, M., Geist, J., 2018. Habitat diversity and connectivity govern the conservation value of restored aquatic floodplain habitats. Biol. Conserv. 217, 1–10. https://doi.org/10.1016/j.biocon.2017.10.024.

Pander, J., Knott, J., Mueller, M., Geist, J., 2019. Effects of environmental flows in a restored floodplain system on the community composition of fish, macroinvertebrates and macrophytes. Ecol. Eng. 132, 75–86. https://doi.org/10.1016/j.ecoleng.2019.04.003.

Pander, J., Nagel, C., Geist, J., 2021. Integration of constructed floodplain ponds into nature-like fish passes supports fish diversity in a heavily modified water body. Water 13, 1018. https://doi.org/10.3390/w13081018.

Pander, J., Casas-Mulet, R., Geist, J., 2023. Contribution of a groundwater-influenced hinterland drainage system to the restoration of salmonid spawning grounds at the upper river Danube. Front. Environ. Sci. 11, 1124797 https://doi.org/10.3389/fenvs.2023.1124797.

Parmentier, B., McGill, B.J., Wilson, A.M., Regetz, J., Jetz, W., Guralnick, R., Tuanmu, M.-N., Schildhauer, M., 2015. Using multi-timescale methods and satellite-derived land surface temperature for the interpolation of daily maximum air temperature in Oregon. Int. J. Climatol. 35 (13), 3862–3878. https://doi.org/10.1002/joc.4251.

Piatka, D.R., Venkiteswaran, J.J., Uniyal, B., Kaule, R., Gilfedder, B., Barth, J.A., 2022. Dissolved oxygen isotope modelling refines metabolic state estimates of stream ecosystems with different land use background. Sci. Rep. 12 (1), 10204 https://doi.org/10.1038/s41598-022-13219-9.

Piggott, J.J., Townsend, C.R., Matthaei, C.D., 2015. Climate warming and agricultural stressors interact to determine stream macroinvertebrate community dynamics. Glob. Chang. Biol. 21 (5), 1887–1906. https://doi.org/10.1111/gcb.12861.

Poff, N.L., Brinson, M.M., Day, J.W., 2002. Aquatic Ecosystems and Global Climate Change. Pew Center on Global Climate Change, Arlington, VA, USA, pp. 1–36.

Poole, G.C., Stanford, J.A., Running, S.W., Frissell, C.A., 2006. Multiscale geomorphic drivers of groundwater flow paths: subsurface hydrologic dynamics and hyporheic habitat diversity. J. N. Am. Benthol. Soc. 25, 288–303. https://doi.org/10.1899/0887-3593(2006)25[288:MGDOGF]2.0.CO;2.

Pörtner, H.O., Peck, M.A., 2010. Climate change effects on fishes and fisheries: towards a cause-and-effect understanding. J. Fish Biol. 77 (8), 1745–1779. https://doi.org/10.1111/j.1095-8649.2010.02783.x.

Powers, P.D., Helstab, M., Niezgoda, S.L., 2019. A process-based approach to restoring depositional river valleys to stage 0, an anastomosing channel network. River Res. Appl. 35 (1), 3–13. https://doi.org/10.1002/rra.3378.

Powers, P., Staab, B., Cluer, B., Thorne, C., 2022. Rediscovering, reevaluating, and restoring Entiatqua: identifying pre-Anthropocene valleys in North Cascadia, USA. River Res. Appl. 38 (9), 1527–1543. https://doi.org/10.1002/rra.4016.

Reid, A.J., Carlson, A.K., Creed, I.F., Eliason, E.J., Gell, P.A., Johnson, P.T.J., Kidd, K.A., MacCormack, T.J., Olden, J.D., Ormerod, S.J., Smol, J.P., Taylor, W.W., Tockner, K., Vermaire, J.C., Dudgeon, D., Cooke, S.J., 2019. Emerging threats and persistent conservation challenges for freshwater biodiversity. Biol. Rev. 94, 849–873. https://doi.org/10.1111/brv.12480.

Sawyer, A.H., Cardenas, M.B., 2012. Effect of experimental wood addition on hyporheic exchange and thermal dynamics in a losing meadow stream. Water Resour. Res. 48 https://doi.org/10.1029/2011WR011776.

Siegel, J.E., Fullerton, A.H., Jordan, C.E., 2022. Accounting for snowpack and time-varying lags in statistical models of stream temperature. J. Hydrol. 17, 100136 https://doi.org/10.1016/j.hydroa.2022.100136.

Skidmore, P., Wheaton, J., 2022. Riverscapes as natural infrastructure: meeting challenges of climate adaptation and ecosystem restoration. Anthropocene 38, 100334. https://doi.org/10.1016/j.ancene.2022.100334.

Smialek, N., Pander, J., Geist, J., 2021. Environmental threats and conservation implications for Atlantic salmon and brown trout during their critical freshwater phases of spawning, egg development and juvenile emergence. Fish. Manag. Ecol. 28, 437–467. https://doi.org/10.1111/fme.12507.

Smith, L.L., Smith, L.L., Koenst, W.M., 1975. Temperature Effects on Eggs and Fry of Percoid Fishes. National Environmental Research Center, Washington.

Stammel, B., Cyffka, B., Geist, J., Mueller, M., Pander, J., Blasch, G., Fischer, P., Gruppe, A., Haas, F., Kilg, M., Lang, P., Schopf, R., Schwab, A., Utschik, H., Weißbrod, M., 2012. Floodplain restoration on the Upper Danube (Germany) by re-establishing water and sediment dynamics: a scientific monitoring as part of the implementation. River Systems 20, 55–70. https://doi.org/10.1127/1868-5749/2011/020-0033.

Steel, E.A., Beechie, T.J., Torgersen, C.E., Fullerton, A.H., 2017. Envisioning, quantifying, and managing thermal regimes on river networks. BioScience 67 (6), 506–522. https://doi.org/10.1093/biosci/bix047.

Sullivan, K., Martin, D.J., Cardwell, R.D., Toll, J.E., Duke, S., 2000. An Analysis of the Effects of Temperature on Salmonids of the Pacific Northwest with Implications for Selecting Temperature Criteria. Sustainable Ecosystems Institute, Portland, OR.

Thorp, J.H., Thoms, M.C., Delong, M.D., 2006. The riverine ecosystem synthesis: biocomplexity in river networks across space and time. River Res. Appl. 22, 123–147. https://doi.org/10.1002/rra.901.

Tonolla, D., Acuna, V., Uehlinger, U., Frank, T., Tockner, K., 2010. Thermal heterogeneity in river floodplains. Ecosystems 13, 727–740. https://doi.org/10.1007/s10021-010-9350-5.

Torgersen, C.E., Price, D.M., Li, H.W., McIntosh, B.A., 1999. Multiscale thermal refugia and stream habitat associations of Chinook salmon in northeastern Oregon. Ecol. Appl. 9 (1), 301–319. https://doi.org/10.1890/1051-0761(1999)009[0301:MTRASH]2.0.CO;2.

Torgersen, C., Ebersole, J., 2012. Primer for identifying cold-water refuges to protect and restore thermal diversity in riverine landscapes. EPA Sci. Guid. Handb. 91 (doi:EPA 910-c-12-001)f.

Torgersen, C.E., Faux, R.N., McIntosh, B.A., Poage, N.J., Norton, D.J., 2001. Airborne thermal remote sensing for water temperature assessment in rivers and streams. Remote Sens. Environ. 76 (3), 386–398. https://doi.org/10.1016/S0034-4257(01)00186-9.

Van Vliet, M.T.H., Franssen, W.H.P., Yearsley, J.R., Ludwig, F., Haddeland, I., Lettenmaier, D.P., Kabat, P., 2013. Global river discharge and water temperature under climate change. Glob. Environ. Chang. 23, 450–464. https://doi.org/10.1016/j.gloenvcha.2012.11.002.

Vörösmarty, C.J., McIntyre, P.B., Gessner, M.O., Dudgeon, D., Prusevich, A., Green, P., Glidden, S., Bunn, S.E., Sullivan, C.A., Liermann, C.R., Davies, P.M., 2010. Global threats to human water security and river biodiversity. Nature 467, 555–561. https://doi.org/10.1038/nature09440.

Wawrzyniak, V., Piégay, H., Allemand, P., Vaudor, L., Grandjean, P., 2013. Prediction of water temperature heterogeneity of braided rivers using very high resolution thermal infrared (TIR) images. Int. J. Remote Sens. 34 (13), 4812–4831. https://doi.org/10.1080/01431161.2013.782113.

Webb, B.W., Hannah, D.M., Moore, R.D., Brown, L.E., Nobilis, F., 2008. Recent advances in stream and river temperature research. Hydrological Processes: An International Journal 22 (7), 902–918. https://doi.org/10.1002/hyp.6994.

Weber, N., Bouwes, N., Pollock, M.M., Volk, C., Wheaton, J.M., Wathen, G., Wirtz, J., Jordan, C.E., 2017. Alteration of stream temperature by natural and artificial beaver dams. PloS One 12 (5), e0176313. https://www.ncbi.nlm.nih.gov/pubmed/28520714.

White, J.C., Khamis, K., Dugdale, S., Jackson, F.L., Malcolm, I.A., Krause, S., Hannah, D. M., 2023. Drought impacts on river water temperature: A process-based understanding from temperate climates. Hydrol. Process. 37 (10), e14958 https://doi.org/10.1002/hyp.14958.

Wilby, R.L., Orr, H., Watts, G., Battarbee, R.W., Berry, P.M., Chadd, R., Dugdale, S.J., Dunbar, M.J., Elliott, J.A., Extence, C., Hannah, D.M., Holmes, N., Johnson, A.C., Knights, B., Milner, N.J., Ormerod, S.J., Solomon, D., Timlett, R., Whitehead, P.J., Wood, P.J., 2010. Evidence needed to manage freshwater ecosystems in a changing climate: turning adaptation principles into practice. Sci. Total Environ. 408, 4150–4164. https://doi.org/10.1016/j.scitotenv.2010.05.014.

Wild, R., Nagel, C., Geist, J., 2023. Climate change effects on hatching success and embryonic development of fish: assessing multiple stressor responses in a large-scale mesocosm study. Sci. Total Environ. 893, 164834 https://doi.org/10.1016/j.scitotenv.2023.164834.

Wohl, E., 2016. Spatial heterogeneity as a component of river geomorphic complexity. Progress in Physical Geography: Earth and Environment 40, 598–615 (doi:10.1177/0309133316658615).

Wohl, E., Castro, J., Cluer, B., Merritts, D., Powers, P., Staab, B., Thorne, C., 2021. Rediscovering, reevaluating, and restoring lost riverwetland corridors. Front. Earth Sci. 9, 653623 https://doi.org/10.3389/feart.2021.653623.

Wood, S.N., 2011. Fast stable restricted maximum likelihood and marginal likelihood estimation of semiparametric generalized linear models. *Journal of the Royal Statistical Society*. Series B: Statistical Methodology 73, 3–36. https://doi.org/10.1111/j.1467-9868.2010.00749.x.

Zuur, A.F., Ineo, E.N., Walker, N.J., Saveliev, A.A., Smith, G.M., 2009. Mixed Effects Models and Extensions in Ecology with R. Springer Science and Business Media, New York, USA, p. 458. https://doi.org/10.1007/978-0-387-87458-6.